Heliyon 7 (2021) e07171

Contents lists available at ScienceDirect

Heliyon

journal homepage: www.cell.com/heliyon

Research article

Theoretical design of D-π-A system new dyes candidate for DSSC application

R. Kacimi [a,*], M. Raftani [b], T. Abram [c], A. Azaid [a], H. Ziyat [b], L. Bejjit [c], M.N. Bennani [b], M. Bouachrine [a,d]

[a] CMC-Molecular Chemistry and Natural Substances Laboratory, Faculty of Sciences, University Moulay Ismail, Meknes, Morocco
[b] Laboratory of Chemistry and Biology Applied to the Environment, Faculty of Sciences, My Ismail University, BP – 11201, Zitoune, Meknes, Morocco
[c] MEM, LASMAR Laboratory, University Moulay Ismail, Meknes, Morocco
[d] EST Khenifra, Sultane Moulay Slimane University, Khenifra, Morocco

ARTICLE INFO

Keywords:
Phenothiazine (PTZ)
DFT
Organic dyes
Dye-sensitized solar cells

ABSTRACT

Currently, dye-sensitized solar cells (DSSCs) are one of the energy technologies that has piqued the interest of researchers, due to their distinct characteristics such as excellent air stability, ease of synthesis and photovoltaic properties interesting. This work aims to study the optoelectronic properties and photovoltaic of six organic dyes based on phenothiazine (PTZ). The effects of bridging core modifications of recently synthesized PSB-4(R) molecule on structural, photovoltaic, electronic, and optical properties of D1-D6 are studied. Using the method Density Functional Theory (DFT) level of the B3LYP (Becke three-parameter Lee–Yang–Parr) exchange correlation functional with 6-31G (d, p) and time-dependent DFT (TD-DFT). According to the obtained results, optoelectronic properties and photovoltaic of the dyes, we can suggest that these designed molecules are better sensitizers as a candidate for the production of dye solar cells (DSSCs). This theoretical study paves the way for chemists to synthesize more efficient sensitizers for applications in dye solar cells.

1. Introduction

The strong growth of developing countries has reflected an increase in global energy consumption estimated at double current demand if policies, in terms of both energy saving and efficiency, are not more proactive. One of the most promising solutions for the future energy of humanity is the development of other forms (of energy) known as "renewable energies". This type of energy has immense advantage of being the natural origin, inexhaustible and non-polluting, since they do not emit greenhouse gases nor radioactive waste. Although solar cells made of silicon achieve yields that vary between 15% and 25.4% [1]. Their manufacturing costs and weight are high. This is an obstacle to their massive use by individuals and manufacturers. New alternatives to reduce the cost of these cells are (DSSCs) or “Grätzel cell”, which is a photoelectrochemical device that converts sunlight into electricity [2, 3]. With a relatively low cost [4, 5, 6, 7] and design that results in a wide range of molecular structures that can be accessed and tunable color [8, 9], their current yield is over 13 % [10]. Iodide/triiodide, electrolytes, and then a platinum counter electrode [11, 12, 13] compared to traditional P–N junction solar cells, they have considerably lower production costs. The most effective organic dyes (DSSCs) have the molecular architecture donor-bridge-acceptor (D–π–A); donors (D) are triarylamine or carbazole. In the literature, we can find many up-to-date examples of various D-π-A compounds based on PTZ framework with various linkers and significant photovoltaic performance [14, 15, 16, 17, 18]. In our study, the phenothiazine group (PTZ) is chosen as a donor while the groups derived from cyanoacrylic acid are considered an acceptor. This push-pull system facilitates the transfer of intramolecular load from the donor group to the acceptor through the π-conjugated units. In the past few years, several research groups provide an effort to improve the properties of D-π-A dyes [19, 20]. The principle of a dye solar cell operation is the absorption of the photosensitizer to the surface of the semiconductor. As light (in the visible spectrum) is absorbed, the dye is excited in its first excited state (S*) and then oxidized as electrons are transferred into the conduction band (CB) of TiO_2, the carboxylic group (COOH) at the end of the dye rings: the COOH forms a bond with the surface of the TiO_2, network, giving it a proton. The oxidized dye is then diminished by a reducing agent and regenerated against the counter-electrode [21]. The separation of charges in (DSSC) is done by a process of electron transfer from the dye to TiO_2, as well as the process of transporting holes from the oxidized dye to the electrolyte. The mechanism of electron transfer is strongly dependent on the electronic structure

* Corresponding author.
E-mail address: r.kacimi@edu.umi.ac.ma (R. Kacimi).

https://doi.org/10.1016/j.heliyon.2021.e07171
Received 14 December 2020; Received in revised form 15 March 2021; Accepted 27 May 2021

of the absorbent dye molecule and the adequacy of energy levels between the excited state of the dye and the CB of the TiO_2. However, the separation of charges is directly related to the positioning of the energy levels between the molecule of the dye and other nanoparticles. The excited state S* of the dye is greater than the limit of the TiO_2 conduction band; and (level 1) of this dye is lower than the chemical potential of the redox iodide/tri-iodide pair (I^-/I_3)in the electrolyte [22]. These two are now an energetic driving force for the separation of electrons and holes. The semiconductor nanoparticle array functions not only as a large substrate surface for the dye molecules, but also as a transport medium for the electrons injected from them.

In another work, we investigate the design of six light-absorbing dyes named Di (i = 1–6) with a donor–π–bridge–acceptor (D-π-A) structure. The optoelectronic properties are calculated using DFT approaches. Then, photovoltaic applications of these designed molecules are related to molecule PSB-4(R) through computational studies.

In this computational study, we have designed six new molecules (D1-D6) after modification in reference molecule synthesized. From the study, the molecules designed exhibit broad absorption bands in the visible region. The calculated parameters include the energy gap, the density of states (DOS), reorganization energies, electron injection driving force (ΔG inject), light-harvesting efficiency (LHE) curve, open-circuit voltage (V_{oc}), natural bond orbital (NBO) analyses, (TDM) analysis, exciting state time, and frontier molecular orbital FMOs. According to the obtained results from these parameters, our work is useful to effectively guide efforts to synthesize these designed molecules (D1-D6) in the discovery of highly efficient (DSSCs).

2. Theoretical methodology

In the current study, we present a theoretical study of optical and electronic properties of the six molecules and the PSB-4(R) (Figure 1). This study has been performed without symmetry restriction on the ground state using DFT at the B3LYP level with the standard 6-31G (d, p) basis in the gas phase (Figure 2). To evaluate the properties, we made use of the Gaussian 09 package [23], with Gauss view 06 for visualization [24]. The spectrum of absorption of designed molecules has been computed through the TD-B3LYP/6-31G (d, p) basis set from the optimization structures. DFT with the Becke three-parameter exchange functional and Lee-Yang-Parr functional (B3LYP) [25, 26, 27, 28] and 6-31G (d, p) [29] have been employed. Electronic transitions (vertical excitation spectra including wavelengths and oscillator strength f), LHE, and electron injection driving force (ΔG^{inject}) of designed molecules are calculated using TD-DFT [30] with method-B3LYP (CAM-B3LYP) [31]. The charge transfer upon electronic transitions has been examined by charge density difference (CDD) and means of the (TDM) implanted in Multiwfn 3.1 [32].

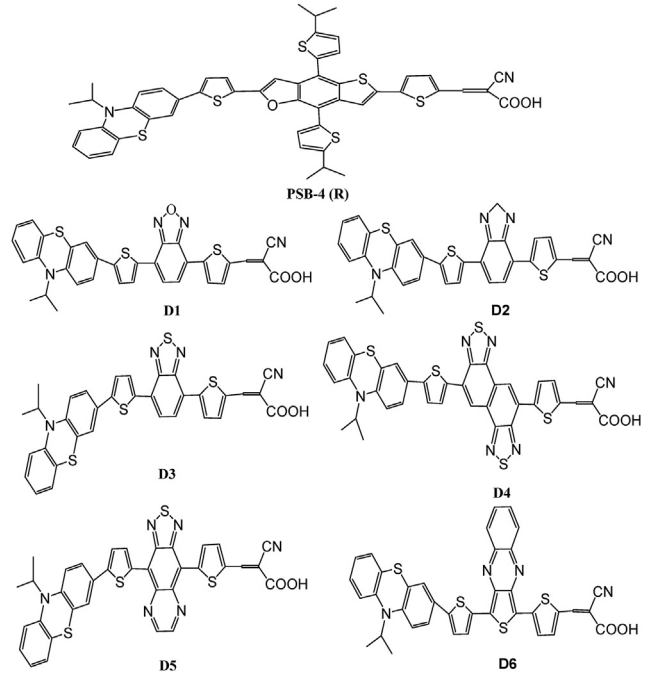

Figure 1. Chemical structure for the PSB-4(R) and designed molecules Di (i = 1–6).

2.1. Frontier molecular analysis and electronic properties

Analysis of electron density distribution over the frontier molecular orbitals across different parts of the studied dyes indicates intramolecular charge transfer (ICT) of the ground state dyes have been performed (Figure 3). The analysis shows that the HOMO's of molecules D1, D2, D3, and D4 are localized in the donor groups phenothiazine (PTZ), while LUMO's are spread on the π-spacers and the central acceptor unit. For the designed molecules D5, D6 and reference (R), the HOMO electrons are largely spread on these molecules with maximum density on donor groups, and with less localization on the acceptor group. The LUMOs are primarily localized at the level of the cyanoacrylic acid units, with maximum density on π-spacers groups for D5 and D6. In contrast, the D1-D6 dyes exhibit a high LUMO charge density. This indicates the formation of a semiconductor electronic dye coupling resulted from high electron injection. These outcomes expose that the π-bridge groups substituted have clear effects on the distribution of (FMOs).

To illustrate the split of the excited state exciton and charge separation, it is useful to investigate the (EDDM) between the excited states and the ground ones. The electron density difference maps (Figure 4) reveal that a load transfer has been performed between the excited states and the ground ones for all the studied dyes. This is because of the

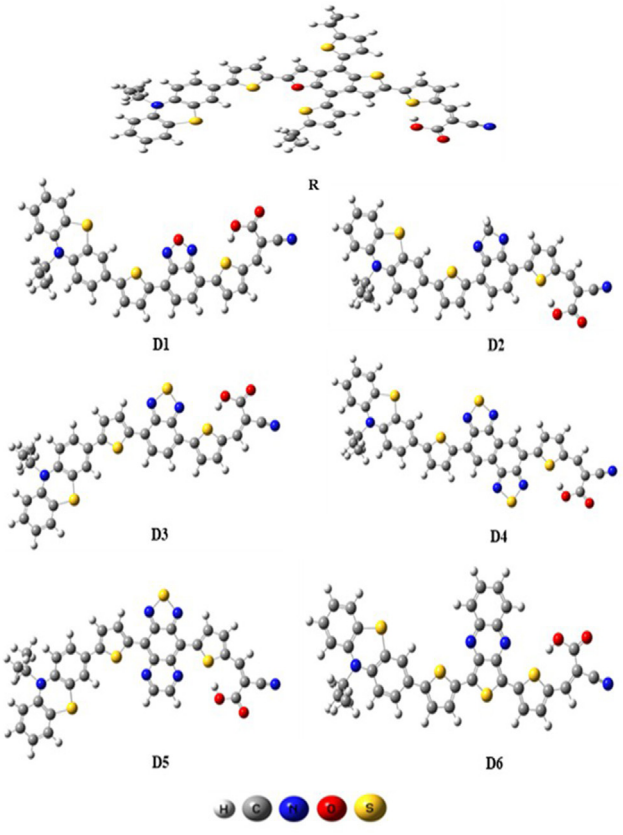

Figure 2. Ground-state optimized geometries of the compounds (D1-D6) and R obtained by B3LYP/6-31G (d, p).

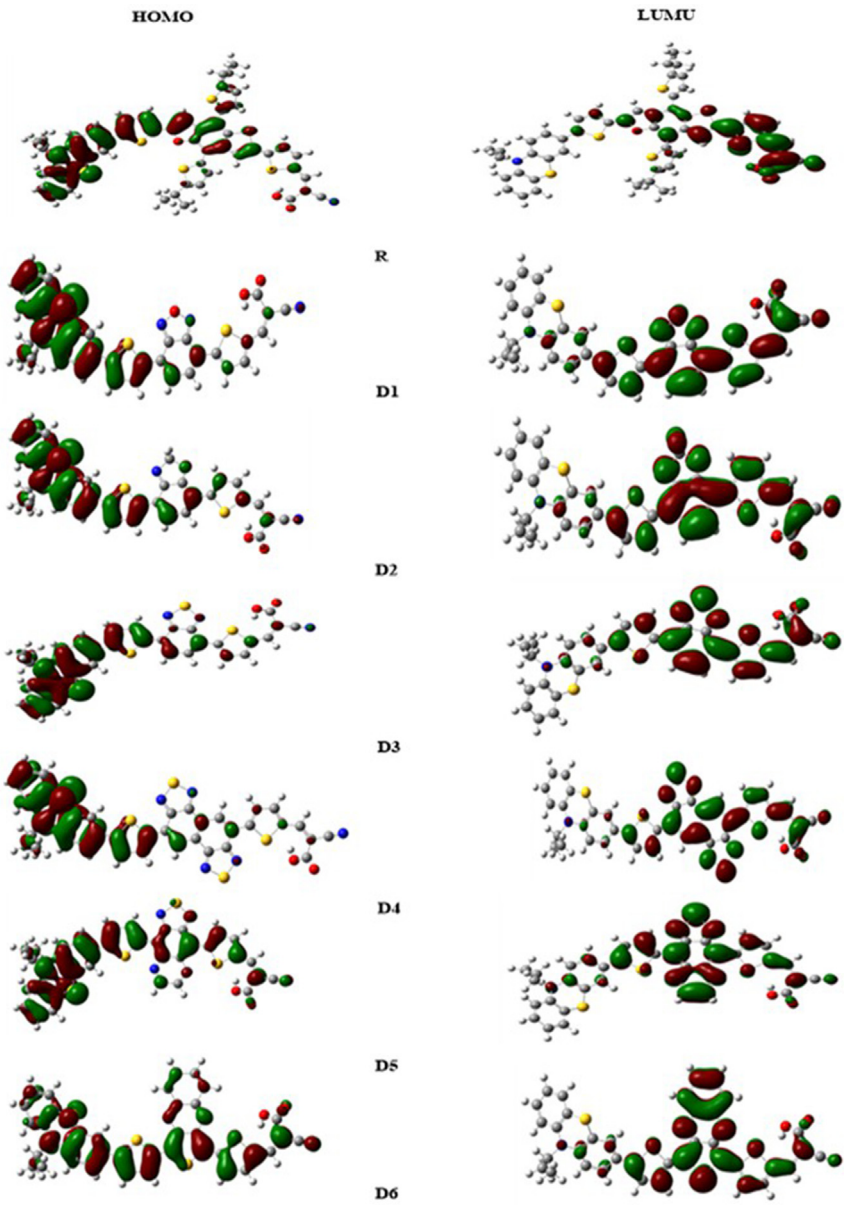

Figure 3. (FMOs) diagram of the molecular orbitals HOMO and LUMO of studied dyes D1-D6 and (R) at B3LYP/6-31G (d, p) level of theory.

electronic charge movement from the phenothiazine (PTZ) to the cyanoacrylic acid. The (EDDM) plots show the decrease of electron density localized on the main electron phenothiazine (PTZ) donor and the π-spacer segments, Additionally, the electron density on the π-linker and the cyanoacrylic acid units increased. For all of the dyes tested. The electron density increment zone (purple) is primarily focused on the acceptor region, with a minor contribution from the π-spacer; however, the electron density (blue) is primarily focused on the donor group, with a minor contribution from the π-spacer for dyes D1-D6. These results indicate that the (ICT) between the excited states and the ground-state have been performed for all the designed dyes and an absorption shift towards the red and a reduction band gap upon light absorption process have been observed, which is essential for an efficient dye-sensitized solar cells.

The E_{HOMO}, E_{LUMO}, and HOMO–LUMO energy gap of all designed molecules and the molecule (R) have been computed in the gas phase from the ground state optimized geometry. Their values are presented in Table 1. The theoretically calculated values of the HOMO and LUMO energies of the reference compound are -4.67 eV and -2.68 eV, while the associated energy gap is 1.99 eV. The experimental HOMO and LUMO energy levels of the reference molecule are -5.07 eV and -2.88 eV, along with the energy band gap (2.19 eV) [33]. It is noted that the theoretically obtained results are in good agreement with those obtained experimentally. These results reflect that the choice of the methods of density theory (DFT) and functional theory of density as a function of time (TD-DFT), cited above, is a good option for predicting the photovoltaic, electronic, and optical properties of the newly designed molecules. The calculated values of the associated energy E_{gap} of the reference molecule show a slight deviation in comparison to those of the experimental values, since our calculation model does not consider the solid-state packing effect of the compounds.

3. Results and discussion

3.1. Structure of studied dyes

In our work, the experimentally synthesized PSB-4(R) is taken as a reference. The structure of the reference molecule consists of

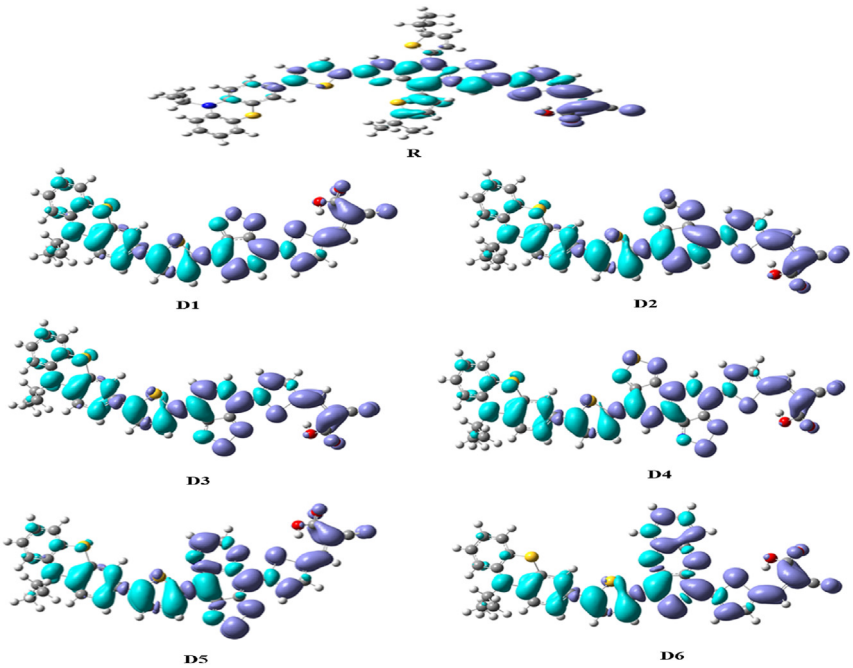

Figure 4. Electron density difference maps between the excited states and the ground ones of dyes Di (i = 1–6) and the reference R.

phenothiazine (PTZ) as donor and cyanoacrylic acid as electron acceptor [25]. We have replaced the terminal 4,8-bis(5-isopropylthiophen-2-yl)-2, 6-dimethylthieno [2,3-f]benzofuran group of the reference molecule with different reported π-spacers (D1-D6) moieties. The chemical structures of the six dyes (Figure 1). By carrying out the above-mentioned π-spacers (D1-D6) modifications in the reference molecule, six distinct dyes are obtained.

It is noticed that all our novel dyes show a narrow energy gap compared to the reference molecule. This means that all the designed molecules exhibit easy charge transfer phenomenon from the ground state to the excited one. In comparison to the reference, this transfer favors efficient electron injection at the conduction band TiO_2. D5 and D6 show the lowest energy gap value among all other designed molecules. This is due to higher extended conjugation in the π-linker segments inserted and the presence of different chromophore units (–C=O, –C=N, and –C–S–C–), in order to make higher aromatic stability through resonance so large charge transfer phenomenon which can be done from the ground state to the excited one. That's why D5 and D6 are recommended as the most effective candidates of the series for applications in organic dye solar cells.

The energy level diagram of the designed compounds D1, D2, D3, D4, D5, D6 and the reference compound R is displayed in Figure 5, along with CB and VB of TiO_2 and the regeneration of the oxidized dyes by I_3^-/I^- redox couple. It is seen that the LUMO values of the compounds D1 to D6 lie sufficiently above the CB edge of TiO_2, providing a required driving force for successful injection of the

Table 1. The energy of HOMOs, LUMOs, and Egap at B3LYP/6–31 G (d, p) level of theory for the compounds Di (i = 1–6) and R. In the parenthesis, the experimental values are given.

Dye	E_{HOMO}	E_{LUMO}	E_{gap}
R	-5.01 (-5.07)	-2.88 (-2.88)	2.13 (2.19)
D1	-5.20	-3.33	1.87
D2	-5.15	-3.40	1.76
D3	-5.20	-3.25	1.96
D4	-5.16	-3.41	1.75
D5	-5.16	-3.73	1.43
D6	-5.03	-3.50	1.53

Table 2. The NBO analysis of all the designed compounds (D1-D6) and reference (R) at B3LYP/6-31G (d,p) level of theory.

dyes	Donating Group	π-spacer	Acceptor Group
R	0.019	0.108	-0.127
D1	0.045	0.058	-0.109
D2	0.045	0.083	-0.123
D3	0.037	0.083	-0.120
D4	0.035	0.076	-0.114
D5	0.064	0.067	-0.131
D6	0.045	0.110	-0.155

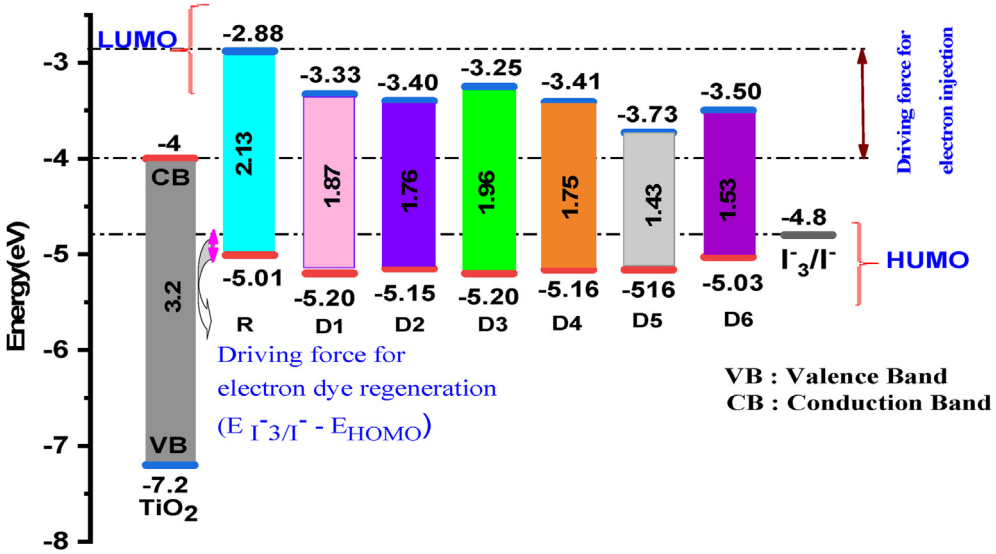

Figure 5. Energy level plot of the designed compounds D1 to D6 and R.

electrons from the LUMO (excited-state) of the dye to the CB TiO_2. It is also worth noting that the HOMO energy level of all engineered molecules is lower than the redox energy level of the I_3^-/I^- redox shuttle. So, the impede back-electron transfer from the conduction band of TiO_2 to the redox energy level of the redox shuttle (the recombination process) cannot be performed.

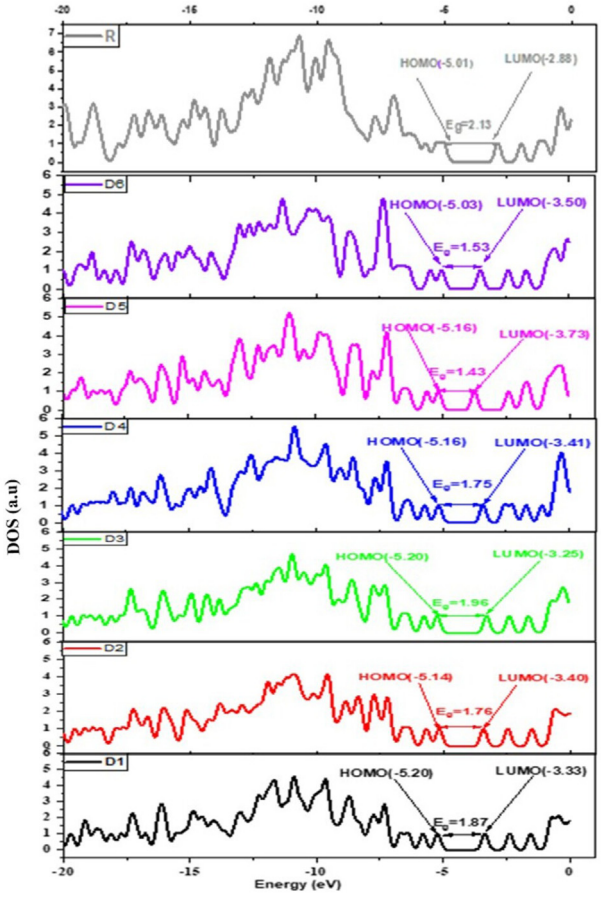

Figure 6. Density of states for the studied dyes D1-D6 and (R) at B3LYP/6-31G (d,p) level of theory.

3.2. Milliken's population analysis

In order to learn more, density distribution over the (FMOs) [34], a density of states (DOS) investigation has also been accomplished by DFT/B3LYP/6-31G (d, p) method. The outcomes from the DOS involvement (Figure 6) support the evidence revealed by the FMOs in (Figure 3). The density of states of the spectrum represents that HOMO density significantly spreads on the donor moiety and slightly on the π-linker group, while LUMO is contributed by the acceptor and π-linker moieties. The density of the state's spectrum indicates that the effect of the bridge group on distribution pattern is seen in DOS spectra. The major contribution of bridge groups in D5 and D6 towards FMOs is seen compared to other bridge groups. This analysis also predicts that there is a significant delocalization of electron density. Also, a significant amount of charge transfer occurs from the donor group to acceptor regions.

3.3. NBO analysis

In molecular systems, the (NBO) analysis is a critical parameter for examining charge transfer or conjugative interaction. It also provides a convenient platform for researching intramolecular and intermolecular bonding, as well as interactions between bonds [35].

To compare the partial charges on the donor moiety (phenothiazine), group π-spacers (bridge), and acceptor moiety (cyanoacrylic acid); the calculation of NBO has been carried out using the B3LYP/6-31G (d, p) method in the gas phase (Table 2). It is noted that all the molecules have positive charges that are situated in the donor part and the π-spacers part, while the negative charges are located in the acceptor part. Contrarily, the positive charges in the bridge inserted demonstrate that this unit behaves as a donor. The most positive charge on the donor of the compound D5 and the π-spacer for D6 is the indication of being the most effective electron donor, while the highest negative (NBO) charge for all the studied dyes is located on the acceptor moiety which acts as the best acceptor moiety. The Natural bond orbital analysis demonstrates the charge-separated state generated in the dye molecule and proves that the charge transfer can be produced between donor and acceptor moieties.

3.4. Simulated Uv-visible absorption spectra

The UV-Visible absorption spectra of the newly designed photovoltaic materials (D1-D6) and the molecule R are computed at the TD-CAM-B3LYP functional with the 6-31G (d,p) basis set as stated in the

Table 3. Computed maximum absorption wavelengths (λ_{max}, in nm), f, and major percentage contribution for all designed dyes D1 to D6 and molecule R using CAM -B3LYP/6-31G (d,p) method in the gas phase.

Dyes	Calcu. λ_{max} (nm)	E_{ex} (eV)	*f*	MO/character	(%)
R	463.35	2.6740	1.5586	HOMO→LUMO	(63%)
	383.12	2.6740	0.4411	HOMO-2 →LUMO	(35%)
	361.22	3.2340	0.7634	HOMO-3→LUMO	(35%)
D1	514.50	2.4081	1.5103	HOMO →LUMO	(63%)
	389.32	3.1824	0.0977	HOMO-1 →LUMO	(58%)
	336.58	3.6810	0.1855	HOMO-1→LUMO+1	(35%)
D2	569.26	2.1765	1.7884	HOMO→LUMO	(66%)
	403.57	3.0701	0.0138	HOMO-1 →LUMO	(59%)
	360.80	3.4340	0.0586	HOMO →LUMO+1	(46%)
D3	511.21	2.0289	1.3967	HOMO →LUMO	(63%)
	379.54	2.0724	0.0246	HOMO-1 →LUMO	(55%)
	347.73	2.8230	0.3830	HOMO-1 →LUMO+1	(39%)
D4	537.59	2.6740	1.4992	HOMO →LUMO	(61%)
	404.05	2.0151	0.0643	HOMO-1 →LUMO	(49%)
	365.79	2.9178	0.2026	HOMO-1 →LUMO+1	(33%)
D5	729.15	1.6992	0.9254	HOMO → LUMO	(85%)
	478.02	2.5919	0.0384	HOMO-1 →LUMO	(77%)
	403.36	3.0717	0.0011	HOMO-8 →LUMO	(81%)
D6	732.38	1.6918	0.8290	HOMO → LUMO	(92%)
	446.12	2.7773	0.2193	HOMO-1 →LUMO	(71%)
	420.73	2.9449	0.6509	HOMO →LUMO+1	(72%)

theoretical methodology. The spectrum of absorption for the molecules (D1-D6) set has been computed in the gas phase (vacuum) from the fully optimized 3-D structure. The corresponding results are tabulated in Table 3 and illustrated in Figure 7. The results obtained with TD-CAM-B3LYP level of theory are very similar to the reference molecules

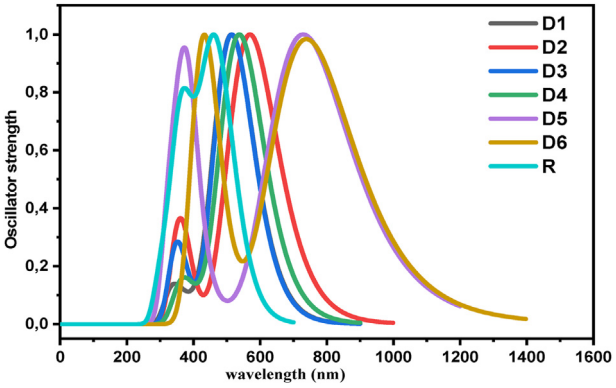

Figure 7. Stimulated absorption spectra of molecules D1-D6 and R in the gas phase using CAM-B3LYP/6-31G (d,p) method.

experimental ultraviolet spectrum [25]. This slight difference between the experimental values and theoretical ones may be attributed to the fact that the theoretical calculation has been carried out in the gas phase, while these experimental values are obtained from the solid-state molecules of dyes. According to Figure 7, the intense absorption peaks are obtained in the visible region. These results are a good argument of the use of organic materials in solar cell devices.

Table 3 presents the recorded maxima absorption values of all the studied molecules. The value of absorption maxima of all designed molecules (D1-D6), the reference R, the oscillator strength (*f*), excitation energies (Eex), and percentage electron transport contributions (%ETC) are theoretically calculated using the method TD-CAM-B3LYP/6-31G (d, p). The theoretical results reveal that the absorption spectra (calculated λ_{max}) of the reference molecule is 484 nm, which is very close to its experimental value 518 nm [33], ensuring a better choice of the used theoretical methods [14, 17]. The molecules absorption spectra show the presence of a large peak between 400 and 1100 nm and narrower peaks in the 250–450 nm wavelength region characterized as a typical $\pi \rightarrow \pi^*$ transition (HOMO to LUMO). These results suggest that all compounds D1 to D6 have only one band in the visible region ($\lambda_{max} > 400$ nm). Among all studied dyes, the highest λmax is exhibited by D5 and D6. This may be due to the increase in the length of conjugation through the π-spacer part. So, the change of the 4,8-bis(5-isopropylthiophen-2-yl)-2,

Table 4. The calculated values of (E_{LUMO} (eV), E_{HOMO} (eV), and V_{OC} (eV), ΔG^{inject}, ΔG_{reg}, and LHE for the dyes D1 to D6 and reference R calculated at DFT/B3LYP/6-31G (d,p).

dyes	E_{HOMO}	E_{LUMO}	E_{00}	E^{dyes}	E^{dyes*}	ΔG^{inject}	ΔG_{reg}	LHE	V_{oc}
R	-5.01	-2.88	2.67	5.01	2.34	-1.66	-0.21	0.97	1.12
D1	-5.20	-3.33	2.67	5.20	2.80	-1.2	-0.40	0.97	0.67
D2	-5.15	-3.40	2.14	5.15	2.97	-1.03	-0.35	0.98	0.60
D3	-5.20	-3.25	2.03	5.20	3.17	-0.83	-0.40	0.96	0.75
D3	-5.16	-3.41	2.02	5.16	2.49	-1.51	-0.36	0.97	0.59
D5	-5.16	-3.73	1.69	5.16	3.46	-0.54	-0.36	0.88	0.27
D6	-5.03	-3.50	2.02	5.03	3.33	-0.67	-0.23	0.85	0.50
TiO_2	-7.2	-4							

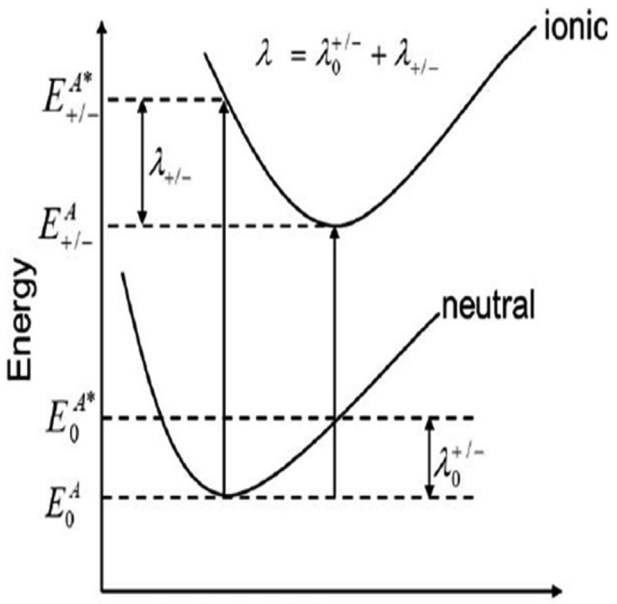

Figure 8. Energies of the neutral compounds at the ground state and the cationic (anionic) systems.

6-dimethylthieno [2,3-f] benzofuran unit by the different π-spacers particularly for molecules D5 and D6 increases the maximum absorption wavelength. Notably, compared to D5 and D6, the compound D4 has a maximum absorption shifted by about 200 nm towards shorter wavelength than D5 and D6. This may be due to a result of the more electron deficient nature of the naphtho [1,2-c:5,6-c']bis ([1,2,5]thiadiazole) acceptor, their planar and rigid backbones usually indicate a close intermolecular interaction [36]. This shows that the designed molecules have excellent absorption properties as compared to the reference molecule.

3.5. Overall efficiencies

The performance of DSSC solar cells relates to broader coverage of the sunlight into electricity. The proposed compounds (D1-D6) act as sensitizers in (DSSCs) photovoltaic parameters such as the open-circuit voltage describe these devices (V_{oc}), which can be calculated according to Eq. (1) [37]:

$$V_{oc} = E_{LUMO} - E_{CB} \quad (1)$$

For the designed molecules, the obtained results from the V_{oc} range from 0.27 to 0.75eV (Table 3). These values are sufficient for a better efficient injection of electrons from E_{LUMO} of the dye to the CB of TiO_2. The light-harvesting efficiency (LHE (λ)) can be determined by Eq. (2) [38, 39]:

$$LHE(\lambda) = 1 - 10^{-f} \quad (2)$$

The more negative value of ΔG^{inject} is attributed to a higher driving force for electrons injected into the semiconductor substrate from the dyes excited states. ΔG^{inject} can be calculated from the difference between excited state oxidation potential of the dye molecules CB of the TiO_2. It is determined by Eq. (3) [40, 41]:

$$\Delta G^{inject} = E^{dye*} - E_{CB} \quad (3)$$

where Edye* denotes the potential oxidation energy of the dye in their excited state. It can be obtained from Eq. (4) [42]:

$$E^{dye*} = E^{dye} - E_{\infty} \quad (4)$$

where $E^{dye}$is the ground state oxidation potential of the dye. E_{∞} is the lowest absorption energy associated with the photo-induced (ICT).

Another electrochemical parameter can be optimized to obtain a higher photoelectric conversion. The free energy of the regeneration of the dye (ΔG_{reg}) can be calculated by Eq. (5) [43]:

$$\Delta G_{reg} = E^{dye}_{ox} - E^{I^-}/_{I_3^-} \quad (5)$$

where$E^{dye}_{ox}$is defined as the ground state oxidation potential and is equal to the negative value of the HOMO energy of the isolated dyes, and I^-/I_3^- is the iodide/tri-iodide redox potential (−4.8 eV) [44]. Table.4 shows that the findings driving force (ΔG^{inject}) of the designed dyes are negative. ΔG^{inject} is shown to be -1.2, -1.03, -0.83, -1.51, -0.54, and -0.67, for Di (i = 1–6), respectively. This predicts spontaneous electron injection from the excited dye molecules to the CB edge of the TiO_2. It is also noted that the designed molecules demonstrate thermodynamically favorable regeneration ability as all ΔG_{reg} values are negative. This means that the dyes excited state is lower than its potential of the I^-/I^-_3 redox couple.

Table.4 shows that the oscillator strengths are 1.5103, 1.7884, 1.3967, 1.4992, 0.9254, and 0.8290 for D1, D2, D3, D4, D5, and D6, respectively. Therefore, the calculated LHE is in the order: D2>D1 = D4 = R > D3> D5> D6. This shows that our entire novel designed molecules have the highest solar light utilization efficiency compared to reference molecule to obtain the higher Jsc.

The reorganization energy λ_{total} has great importance to evaluate the energy penalty resulted from the molecular arrangement that occurs during photoexcitation. Therefore, the calculation of λ_{total} is also important to analyze the kinetics of electron injection from the LUMO (excited state) of the dye to the CB of TiO_2. Marcus semiclassical theory (Eq. (6)) depicts the rate of electron transfer (K_{ET}), which is dependent on the λ_{total}. The relation between them is given in Eq. (6) [45]:

$$\kappa_{ET} = \frac{1}{\sqrt{\lambda_{Total}}}\sqrt{\frac{\pi}{\hbar^2 K_B T}}/V^2 \exp\left\{-\frac{\lambda_{Total}}{4K_B T}\right\} \quad (6)$$

where K_B denotes Boltzmann constant; ħ is the Planks' constant, V represents the electronic coupling constant between initial states and final ones, and T is the absolute temperature. This shows that the electron transfer rate constant K_{ET} depends only on λ_{total} which is a sum of the electron (λe) and hole (λh) reorganization energies whose values can be estimated from (Figure 8) [46] and calculated by Eqs. (7) and (8) respectively [47]:

Table 5. Reorganization energies, λ_{total} values (eV) and excited-state lifetime t (ns) of the designed molecules (D1-D6) and R.

dyes	λ_e	λ_h	λ_{total}	t (ns)
R	0.32	0.25	0.57	0.14
D1	0.33	0.31	0.64	0.17
D2	0.32	0.31	0.63	0.18
D3	0.31	0.31	0.62	0.26
D4	0.26	0.29	0.55	0.14
D5	0.25	0.33	0.59	0.56
D6	0.27	0.32	0.60	0.62

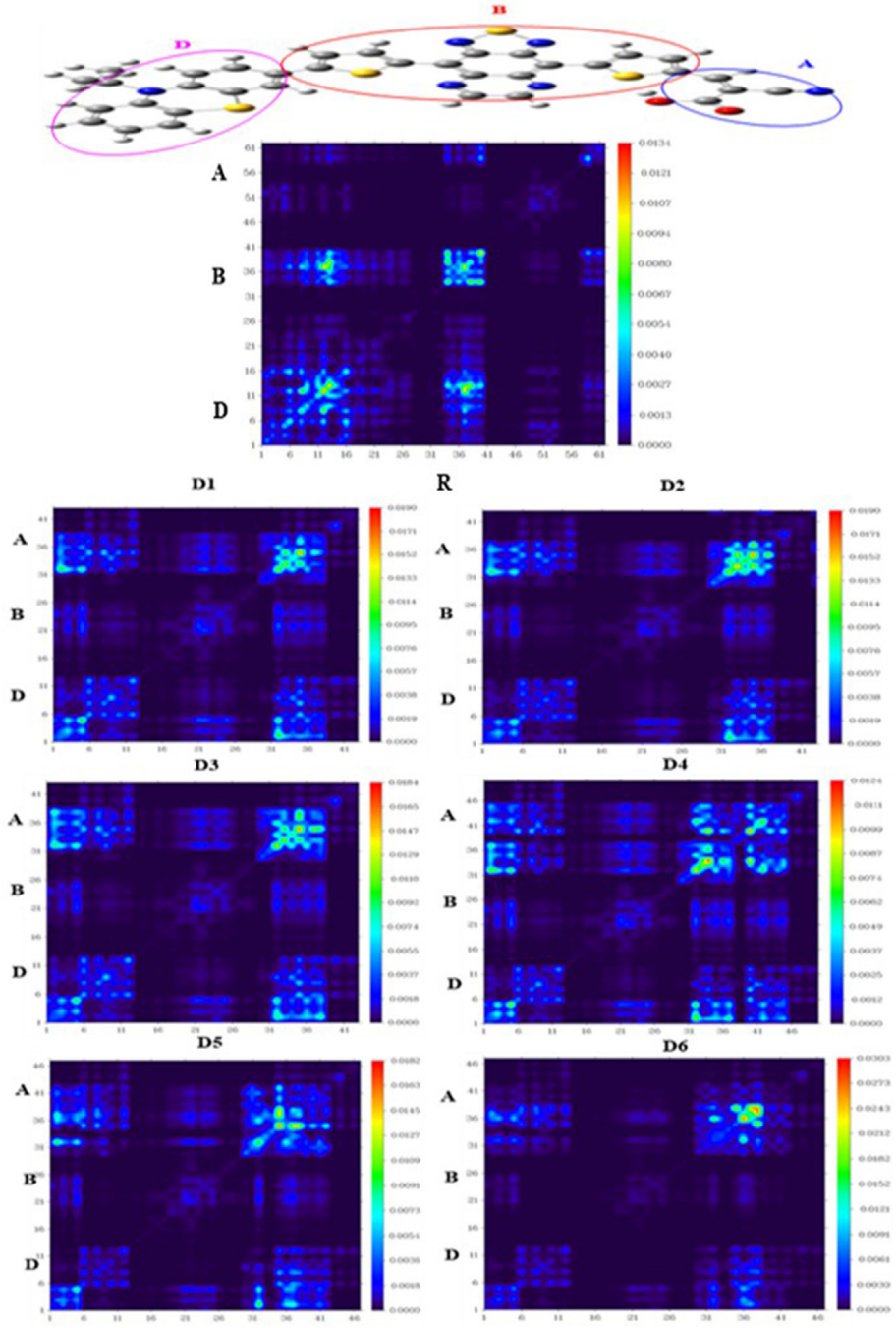

Figure 9. Transition Density Matrix (TDM) of the compounds D1-D6 and R, Donor (D), Acceptor (A) and Bridge (B) calculated at DFT/B3LYP/6-31G (d,p).

$$\lambda_e = \left(E_-^0 - E_0^0\right) - \left(E_0^- - E_-^-\right) \quad (7)$$

$$\lambda_h = \left(E_+^0 - E_0^0\right) - \left(E_0^+ - E_+^+\right) \quad (8)$$

where E_-^0e and E_+^0 denote the energy of the neutral molecule in the optimized anionic (cationic) geometry,E_0^0 represents the energy of the neutral molecule at the ground state, and $E_-^-$and $E_+^+$are the energy of anionic and cationic calculated from the optimized anion (cation) geometry, respectively. For low reorganization energies, charge transfer is fast and efficient.

The rate of charge transfer increases with the decreasing of the reorganization energy λ_{total}. According to the results obtained all the dyes Di (i = 1–6) exhibit low reorganizational energy. Therefore, the dyes (D1-D6) have greater electron transportability between the cyanoacrylic acid (acceptor) and phenothiazine (PTZ) (donor) moieties. The calculated λ_{total} of the compounds are closer and more increased in order: D4< R < D5 < D6 < D3< D2< D1. Therefore, there is an almost equal load transfer capacity. D4, D5, and D6 possess the lowest λ_{total}. The lower dye regeneration driving force and high negative NBO charge on the cyanoacrylic acid moiety affect the photovoltaic performance of D4, D5 and D6. The dye D1 has the largest λ_{total}. As a result, dyes D4, D5, and D6 exhibit a favorable J_{sc} that can be used for future efficient OSCs.

Excited-state lifetime (t) has an important influence on the charge transfer properties of the material. In comparison to the reference molecule, the dyes are engineered to have a longer excited state lifetime. Therefore, the cationic form of the dye molecule remains the most favorable state for efficient charge transfer. The lifetime can be calculated by Eq. (9) [48]:

Table 6. Calculated energy gap E_{gap}, first singlet excitation energy (E_{opt}), and the exciton binding energies (E_b).

dyes	E_{gap} (eV)	E_{opt} (eV)	E_b (eV)
R	2.13	1.93	0.20
D1	1.87	1.77	0.10
D2	1.76	1.62	0.14
D3	1.96	1.79	0.17
D4	1.75	1.71	0.04
D5	1.43	1.12	0.31
D6	1.53	1.15	0.38

$$\tau = \frac{1.499}{fE_{ex}^2} \quad (9)$$

where f denotes the oscillator strength of the excited state and E_{ex} represents the excitation energy, Table 5 shows the lifetime of the excited states with the order of D6 > D5 >D3 > D2 > D1> R = D4, which means that the insertion of novel π-spacers group increases conjugated length. This is helpful to increase the lifetime of excited states compared to the introduction of 4,8-bis(5-isopropylthiophen-2-yl)-2,6 dimethylthieno [2,3-f] benzofuran unit.

3.6. Transition density matrix (TDM)

The (TDMs) analysis is a technique for deciphering and understanding electronic transformation processes in dye-sensitized solar cells [49, 50, 51]. In fact, this parameter provides information on the distribution of the interactions between donor group and acceptor, and also on the linked electron-hole pairs and identify their delocalization and coherence lengths [52]. The method DFT with 6-31G (d, p) level has been used to examine the TDM diagrams of all molecules. To eliminate the complications, we divided the dyes into three parts: Donor (D), Acceptor (A), and Bridge (B), (Figure 9).

According to the TDM diagrams, it can be seen that the designed molecules D1-D6 have a uniform distribution of electrons throughout the molecule. Coherence successfully passes from the donor to the acceptor unit with an effective contribution to the bridge unit, which acts as a facilitator for the transfer of electrons without trapping them. The order of interaction coefficient of the studied molecule between the donor and acceptor parts is D4 < D1< D2< D3< R < D5< D6. This order of transition density matrixes analysis provides evidence that newly designed dyes D5 and D6 show better results than the other molecules.

Exciton binding energy (E_b), which can be used to judge the exciton ability to dissociate, is a crucial parameter for estimating the optoelectronic properties of (DSSCs) [52, 53, 54, 55]. For the dyes (D1-D6), the energy E_{gap} is defined as the difference between the energies of HOMO and LUMO orbitals, while the optical gap energy is the first excited state energy. Binding energy Eb of the electron-hole pair of designed molecules D1 to D6 can be calculated with the help of Eq. (10) [56, 57, 58].

$$E_b = E_{LUMO-HOMO} - E_{opt} \quad (10)$$

According to the results expressed in Table 6, the designed molecule D4 has lower exciton binding energy (E_b) than the other molecules. This means that all molecules exhibit an important charge transfer rate. Consequently, a high current charge density (Jsc) is compared to the other molecules. Besides, the sequence of the E_b values for the designed dyes is D4 < D1< D2< D3< R < D5< D6. These results are in line with previous findings (TDMs) analysis.

4. Conclusion

In this work, we have designed and studied new six dyes D-π-A type and studied for photovoltaic applications by employing the DFT functional and TD-DFT with a 6–31 G (d, p) basis. The designed molecules contain phenothiazine (PTZ) and cyanoacrylic acid by substituting different π-spacer groups at the peripheral sites of PSB-4(R) to examine the bridge effect units on the photovoltaic performance of solar energy driven devices. The designed molecules show a reduction in the energy gap (1.43–1.96 eV). The maximum absorption (732 nm and 729) has been observed for the molecules D6 and D5 with the lowest E_{gap} (1.53 eV and 1.43eV) due to the insertion effect of the different π-spacers. Besides, the molecules D5 and D6 have the highest excited-state lifetime (t) compared to the other molecules. In addition, our designed dyes are good for electron mobility, because the binding energy (E_b) of the-designed molecules (D1 to D6) is lower than the synthesized reference molecule, which is in agreement with the results of the transition density matrix (TDM). Based on this study, the modifications π-spacer groups of the molecule reference affect the performance of designed dyes. In a nutshell, the newly designed dyes D1-D6, especially D5 and D6, should be synthesised in order to create highly effective dye-sensitized solar cells (DSSCs).

Declarations

Author contribution statement

R. Kacimi: Performed the experiments; Analyzed and interpreted the data; Wrote the paper.

M. Raftani, T. Abram, A. Azaid, H. Ziyat: Analyzed and interpreted the data.

M. Bouachrine: Conceived and designed the experiments; Wrote the paper.

L. Bejjit, M. N. Bennani: Contributed reagents, materials, analysis tools or data.

Funding statement

This research did not receive any specific grant from funding agencies in the public, commercial, or not-for-profit sectors.

Data availability statement

Data included in article/supp. material/referenced in article.

Declaration of interests statement

The authors declare no conflict of interest.

Additional information

No additional information is available for this paper.

Acknowledgements

We are grateful to the "Association Marocaine des Chimistes Theoriciens" (AMCT) for its pertinent help concerning the programs.

References

[1] B. Chen, et al., Grain engineering for Perovskite/silicon monolithic tandem solar cells with efficiency of 25.4%, Joule 3 (1) (2019) 177–190.
[2] S. Dheivamalar, K.B. Banu, A DFT study on functionalization of acrolein on Ni-doped (ZnO)6 nanocluster in dye-sensitized solar cells, Heliyon 5 (12) (2019), e02903.
[3] A. El Assyry, M. Lamsayah, I. Warad, R. Touzani, F. Bentiss, A. Zarrouk, Theoretical investigation using DFT of quinoxaline derivatives for electronic and photovoltaic effects, Heliyon 6 (3) (2020), e03620.
[4] B. Chen, et al., Alternative energy technologies, Nature 414 (1) (2001) 332–337.
[5] P. Wang, S.M. Zakeeruddin, J.E. Moser, M.K. Nazeeruddin, T. Sekiguchi, M. Grätzel, Erratum: a stable quasi-solid-state dye-sensitized solar cell with an amphiphilic ruthenium sensitizer and polymer gel electrolyte, Nat. Mater. 2 (7) (2003) 498.
[6] A. Hagfeldt, G. Boschloo, L. Sun, L. Kloo, H. Pettersson, Dye-Sensitized Solar Cells, 2010, pp. 6595–6663.
[7] T.W. Hamann, R.A. Jensen, A.B.F. Martinson, H. Van Ryswyk, J.T. Hupp, Advancing beyond current generation dye-sensitized solar cells, Energy Environ. Sci. 1 (1) (2008) 66–78.
[8] M. Liang, J. Chen, Arylamine organic dyes for dye-sensitized solar cells, Chem. Soc. Rev. 42 (8) (2013) 3453–3488.

[9] Y. Wu, W. Zhu, "Organic sensitizers from D–π–A to D–A–π–A: effect of the internal electron-withdrawing units on molecular absorption, energy levels and photovoltaic performances, Chem. Soc. Rev. 42 (5) (2013) 2039–2058.

[10] L. Zhang, et al., 13.6% efficient organic dye-sensitized solar cells by minimizing energy losses of the excited state, ACS Energy Lett. 4 (4) (2019) 943–951.

[11] G. Wang, et al., Enhanced photovoltaic response of PVK/C60 composite films, Phys. B Condens. Matter 279 (1–3) (2000) 116–119.

[12] S. Kim, et al., Molecular engineering of organic sensitizers for solar cell applications, J. Am. Chem. Soc. 128 (51) (2006) 16701–16707.

[13] S. Ando, et al., Physical properties and field-effect transistors based on novel thiazolothiazole/heterocyclic and thiazolothiazole/phenylene co-oligomers, Synth. Met. 156 (2–4) (2006) 327–331.

[14] N. Duvva, S. Prasanthkumar, L. Giribabu, Influence of strong electron donating nature of phenothiazine on A3B- type porphyrin based dye sensitized solar cells, Sol. Energy 184 (April) (2019) 620–627.

[15] S. Ramasamy, M. Boopathy, S. Johnsanthoshkumar, K. Subramanian, Structural engineering of poly-(methacrylate) bearing push-pull type pendants oxindole-phenothiazine with tetrazole anchoring acceptor for efficient organic photovoltaic cells, Polymer 115 (2017) 128–136.

[16] A. Slodek, D. Zych, G. Szafraniec-Gorol, P. Gnida, M. Vasylieva, E. Schab-Balcerzak, Investigations of new phenothiazine-based compounds for dye-sensitized solar cells with theoretical insight, Materials 13 (10) (2020).

[17] A. Slodek, D. Zych, S. Golba, S. Zimosz, P. Gnida, E. Schab-Balcerzak, Dyes based on the D/A-acetylene linker-phenothiazine system for developing efficient dye-sensitized solar cells, J. Mater. Chem. C 7 (19) (2019) 5830–5840.

[18] A.F. Buene, N. Uggerud, S.P. Economopoulos, O.R. Gautun, B.H. Hoff, "Effect of π-linkers on phenothiazine sensitizers for dye-sensitized solar cells, Dyes Pigments 151 (2018) 263–271. November 2017.

[19] S. Ahmad, E. Guillén, L. Kavan, M. Grätzel, M.K. Nazeeruddin, Metal free sensitizer and catalyst for dye sensitized solar cells, Energy Environ. Sci. 6 (12) (2013) 3439–3466.

[20] Y. Ooyama, Y. Harima, Photophysical and electrochemical properties, and molecular structures of organic dyes for dye-sensitized solar cells, ChemPhysChem 13 (18) (2012) 4032–4080.

[21] J.-M. Yun, Materials chemistry C, J. Mater. Chem. 1 (207890) (2013) 3777.

[22] R. Kacimi, et al., "Computational design of new organic (D–π–A) dyes based on benzothiadiazole for photovoltaic applications, especially dye-sensitized solar cells, Res. Chem. Intermed. 46 (6) (2020) 3247–3262.

[23] M. Frisch, et al., "Gaussian 09, Revision d. 01, Gaussian," Inc. 201, 2009. Wallingford CT.

[24] H. Qin, Application of Gaussian and GaussView in teaching structural chemistry, Guangzhou Chem. Ind. 10 (2012) 83.

[25] R. Kacimi, T. Abram, M. Bourass, L. Bejjit, K. Alimi, M. Bouachrine, "Molecular design of D–A–D conjugated molecules based on fluorene for organic solar cells, Opt. Quant. Electron. 51 (3) (2019).

[26] O. Ninis, R. Kacimi, H. Bouaamlat, M. Abarkan, M. Bouachrine, Theoretical studies of photovoltaic properties for design of new Azo-Pyrrole photo-sensitizer materials as dyes in solar cells, J. Mater. Environ. Sci. 8 (7) (2017) 2572–2578.

[27] R. Kacimi, T. Abram, W. Saidi, L. Bejjit, M. Bouachrine, New organic molecular based on Bis-Dipolar Diphenylamino-EndcappedOligo Aryl Fluorene Application for organic solar cells, Mater. Today Proc. 13 (2019) 1178–1187.

[28] R. Kacimi, T. Abram, L. Bejjit, M. Bouachrine, New organic materiel based on benzothiadiazole for Photovoltaic application Solar Cells, Mater. Today Proc. 13 (2019) 1188–1196.

[29] J.A. Mikroyannidis, D.V. Tsagkournos, P. Balraju, G.D. Sharma, Low band gap dyes based on 2-styryl-5-phenylazo-pyrrole: synthesis and application for efficient dye-sensitized solar cells, J. Power Sources 196 (8) (2011) 4152–4161.

[30] E. Runge, E.K.U. Gross, Density-functional theory for time-dependent systems, Phys. Rev. Lett. 52 (12) (1984) 997.

[31] T. Yanai, D.P. Tew, N.C. Handy, "A new hybrid exchange–correlation functional using the Coulomb-attenuating method (CAM-B3LYP), Chem. Phys. Lett. 393 (1–3) (2004) 51–57.

[32] T. Lu, F. Chen, Multiwfn: a multifunctional wavefunction analyzer, J. Comput. Chem. 33 (5) (2012) 580–592.

[33] J. Liu, et al., Photovoltaic performance of 4,8-Bis(2′-ethylhexylthiophene)thieno [2,3-f]benzofuran-Based dyes fabricated with different donors in dye-sensitized solar cells, ACS Omega 5 (21) (2020) 12440–12450.

[34] M. Ans, J. Iqbal, B. Eliasson, M.J. Saif, H.M.A. Javed, K. Ayub, Designing of non-fullerene 3D star-shaped acceptors for organic solar cells, J. Mol. Model. 25 (5) (2019).

[35] V.K. Rajan, K. Muraleedharan, A computational investigation on the structure, global parameters and antioxidant capacity of a polyphenol, Gallic acid, Food Chem. 220 (2017) 93–99.

[36] M. Wang, et al., Donor-acceptor conjugated polymer based on naphtho[1,2- c:5,6- c]bis[1,2,5]thiadiazole for high-performance polymer solar cells, J. Am. Chem. Soc. 133 (25) (2011) 9638–9641.

[37] W. Sang-aroon, S. Saekow, V. Amornkitbamrung, Density functional theory study on the electronic structure of Monascus dyes as photosensitizer for dye-sensitized solar cells, J. Photochem. Photobiol. Chem. 236 (2012) 35–40.

[38] W. Fan, D. Tan, W. Deng, "Acene-modified triphenylamine dyes for dye-sensitized solar cells: a computational study, ChemPhysChem 13 (8) (2012) 2051–2060.

[39] J. Xu, et al., "Substituent effect on the π linkers in triphenylamine dyes for sensitized solar cells: a DFT/TDDFT study, ChemPhysChem 13 (14) (2012) 3320–3329.

[40] H. Gökce, N. Öztürk, M. Taşan, Y.B. Alpaslan, G. Alpaslan, Spectroscopic characterization and quantum chemical computations of the 5-(4-pyridyl)-1 H-1, 2, 4-triazole-3-thiol molecule, Spectrosc. Lett. 49 (3) (2016) 167–179.

[41] M.N. Tahir, S.H. Mirza, M. Khalid, A. Ali, M.U. Khan, A.A.C. Braga, Synthesis, single crystal analysis and DFT based computational studies of 2, 4-diamino-5-(4-chloro-phenyl)-6-ethylpyrim idin-1-ium 3, 4, 5-trihydroxybenzoate-methanol (DETM), J. Mol. Struct. 1180 (2019) 119–126.

[42] J.B. Asbury, Y.-Q. Wang, E. Hao, H.N. Ghosh, T. Lian, Evidences of hot excited state electron injection from sensitizer molecules to TiO 2 nanocrystalline thin films, Res. Chem. Intermed. 27 (4–5) (2001) 393–406.

[43] H. Liu, L. Liu, Y. Fu, E. Liu, B. Xue, "Theoretical design of D– π–A–A sensitizers with narrow band gap and broad spectral response based on boron dipyrromethene for dye-sensitized solar cells, J. Chem. Inf. Model. 59 (5) (2019) 2248–2256.

[44] J. Preat, A. Hagfeldt, E.A. Perpete, Investigation of the photoinduced electron injection processes for p-type triphenylamine-sensitized solar cells, Energy Environ. Sci. 4 (11) (2011) 4537–4549.

[45] R.A. Marcus, "On the theory of electron-transfer reactions. VI. Unified treatment for homogeneous and electrode reactions, J. Chem. Phys. 43 (2) (1965) 679–701.

[46] A.S. Khazaal, M. Springborg, C. Fan, K. Huwig, Optimizing small conjugated molecules for solar-cell applications using an inverse-design method, J. Mol. Graph. Model. 100 (2020) 107654.

[47] G.R. Hutchison, M.A. Ratner, T.J. Marks, Hopping transport in conductive heterocyclic oligomers: reorganization energies and substituent effects, J. Am. Chem. Soc. 127 (7) (2005) 2339–2350.

[48] P. Ren, C. Sun, Y. Shi, P. Song, Y. Yang, Y. Li, Global performance evaluation of solar cells using two models: from charge-transfer and recombination mechanisms to photoelectric properties, J. Mater. Chem. C 7 (7) (2019) 1934–1947.

[49] M. Ans, J. Iqbal, K. Ayub, E. Ali, B. Eliasson, Spirobifluorene based small molecules as an alternative to traditional fullerene acceptors for organic solar cells, Mater. Sci. Semicond. Process. 94 (2019) 97–106. February.

[50] M. Ans, K. Ayub, I.A. Bhatti, J. Iqbal, Designing indacenodithiophene based non-fullerene acceptors with a donor-acceptor combined bridge for organic solar cells, RSC Adv. 9 (7) (2019) 3605–3617.

[51] M. Ans, J. Iqbal, I.A. Bhatti, K. Ayub, Designing dithienonaphthalene based acceptor materials with promising photovoltaic parameters for organic solar cells, RSC Adv. 9 (59) (2019) 34496–34505.

[52] M. Ans, et al., "Designing three-dimensional (3D) non-fullerene small molecule acceptors with efficient photovoltaic parameters, Chemistry 3 (45) (2018) 12797–12804.

[53] M. Ans, K. Ayub, X. Xiao, J. Iqbal, Tuning opto-electronic properties of alkoxy-induced based electron acceptors in infrared region for high performance organic solar cells, J. Mol. Liq. 298 (2020) 111963.

[54] M. Ans, et al., Designing alkoxy-induced based high performance near infrared sensitive small molecule acceptors for organic solar cells, J. Mol. Liq. 305 (2020) 112829.

[55] M. Ans, J. Iqbal, B. Eliasson, M.J. saif, K. Ayub, Opto-electronic properties of non-fullerene fused-undecacyclic electron acceptors for organic solar cells, Comput. Mater. Sci. 159 (2019) 150–159. December 2018.

[56] B.G. Kim, C.G. Zhen, E.J. Jeong, J. Kieffer, J. Kim, Organic dye design tools for efficient photocurrent generation in dye-sensitized solar cells: exciton binding energy and electron acceptors, Adv. Funct. Mater. 22 (8) (2012) 1606–1612.

[57] A. Dkhissi, Excitons in organic semiconductors, Synth. Met. 161 (13–14) (2011) 1441–1443.

[58] M.E. Köse, Evaluation of acceptor strength in thiophene coupled donor-acceptor chromophores for optimal design of organic photovoltaic materials, J. Phys. Chem. 116 (51) (2012) 12503–12509.